Title
Uncertainty analysis of far-field precipitation from used nuclear fuel

ISBN
9780894487422

Authors
Salazar, A
Fratoni, M
Ahn, J
et al.

Publication Date
2017

Peer reviewed

UNCERTAINTY ANALYSIS OF FAR-FIELD PRECIPITATION FROM USED NUCLEAR FUEL

Alex Salazar[1], Massimiliano Fratoni[1], Joonhong Ahn[1], and Fumio Hirano[2,3]

[1]*University of California, Berkeley, Department of Nuclear Engineering, Berkeley, CA 94720-1730*
[2]*Japan Atomic Energy Agency, Nuclear Fuel Cycle Engineering Laboratories, Tokai-mura, Ibaraki, Japan*
[3] *International Research Institute for Nuclear Decommissioning, Japan*

salazar@berkeley.edu

The safety assessment of a geological repository for used nuclear fuel must ensure that future generations are shielded from radiation from fission products, in particular those released by re-criticality events. An investigation is required to understand whether or not criticality can actually be achieved. In fulfilling this end, this study assesses the uncertainty in the composition and total mass of precipitates forming in the far-field due to variation in transport parameters. The Latin Hypercube Sampling technique is employed to generate an accurate, random distribution of variables employed in the transport model and to assess the uncertainty of attaining a critical mass. The average characteristics of the damaged fuel from the Fukushima Daiichi reactor cores is used as the reference waste form. Results are compared to the minimum critical masses of previous studies to assess the criticality safety margin.

I. INTRODUCTION

The 2011 accident at the Fukushima Daiichi (FD) power station resulted in the damage of almost 250 MT worth of fuel from three different nuclear reactor cores.[1] Although the exact form and configuration of this fuel is not characterized, permanent disposal in a geological repository is eventually necessary, along with assurances that in-situ criticality can be avoided over geological time. An important task in the repository safety assessment is understanding the scenarios in which natural transport processes can contribute the required magnitude of precipitate for a minimum critical mass, as well as evaluating the fissile content of such a precipitate.

It is presumed that packages for the damaged fuel will be engineered to avoid in-canister criticality events by design; therefore, it is assumed that only through the migration of radionuclides from multiple compromised waste packages can underground criticality be achievable. When fissile material accumulates and becomes moderated by groundwater (GW) and rock, positive reactivity feedback mechanisms can lead to self-sustaining chain reactions and rapid fission power generation.[2] If negative feedback mechanisms do not bring neutron multiplication below unity, the energy release can compromise the role of the natural barrier and create a direct pathway for fission products to the biosphere, potentially resulting in a lethal dose.

The conditions for far-field criticality from FD damaged fuel have been examined previously in a parametric study involving specific configurations of fissile material, bedrock, and groundwater.[3] In this study, the minimum critical masses based on the relative content of those three components were evaluated for sandstone and iron-rich rock. However, the necessary transport conditions for such agglomerations were decoupled from the analysis, including the effects of heavily retarded uranium precursors.

When assessing the values of parameters that would be employed in a nuclide transport analysis, variation is observed that would greatly impact the behavior of dissolution, precipitation, diffusion and advection. In past studies, cases would be made to characterize extremes of behavior for either uranium or its precursors with regard to their release at the surface of the engineered barrier system (EBS).[4] However, the approach in this paper is to employ the Latin Hypercube Sampling (LHS) method to characterize far-field depositions within a certain degree of uncertainty. This stratified sampling technique is more convenient than Monte Carlo for using equally significant statistics for fewer samples. LHS also provides a better sense of system variability as its distributes variable samples evenly over the whole sample space.

Using this approach to handle variability, this study will demonstrate the uncertainty of heavy metal precipitation resulting from comprehensively failed damaged fuel canisters in the far field of an abstract repository. A conservative transport model will be employed that probes the upper bound of precipitation for any set of parameters.

Crystalline granite, which is chemically similar to sandstone, is chosen as reference host rock to correlate with findings from [3]. This host medium is examined for its general properties leading to the retardation and dilution of the heavy metals containing fissile material, along with its low hydraulic gradients and reducing environment.[5]

Furthermore, the neutron-absorbing aspects of this rock are lower than that of iron-rich rocks, which will allow the safety margin to be conservatively based on smaller critical masses.

Precipitates on the order of several metric tons and enrichments of at least 1 wt.% will be examined as potentially indicative of criticality. The time frame of investigation is bounded at 100 million years, and any significant data observed before this time will be taken to guide the performance assessment period. If precipitation does not appear indicative of criticality under conservative assumptions, evaluation of criticality risk can be closed and the assessment can be furthered by examining other scenarios or reducing conservatism. Otherwise, suggestions will be made for further investigations.

II. Background

II.A. Model

II.A.1. Scenario

Canisters of FD damaged fuel are emplaced into a repository separated by a set pitch distance, and each is surrounded by a saturated bentonite buffer. Parallel planar fractures of common aperture *2b* intersect the repository with a spacing of one per meter, which is assumed to be large enough to exclude inter-canister effects on transport. A hydraulic gradient drives groundwater throughout the repository. The groundwater immediately infiltrates canisters upon failure and interacts with the fuel, causing dissolution until all uranium disappears at a time T_L.

Nuclides are released from the surface of the waste congruently with the solubility-limited dissolution rate of the UO_2 fuel. At the waste package surface, the nuclides undergo molecular diffusion into the largely impervious, saturated bentonite, or else form a uniform precipitate until the concentration gradient allows for dissolution. Once in the bentonite, no precipitation is assumed to occur. As nuclides diffuse to the surface of the buffer, they immediately infiltrate the alluvial entrances of the planar fractures, which are assumed to be empty and free of any porous filling material.

Nuclides in the fracture are transported by advection (as controlled by the GW velocity) but also undergo matrix infiltration into the host rock. At some distance into the far-field, the environmental conditions are assumed to promote insolubility and mass accumulation. All fractures lead directly to this point of precipitation, allowing the mass fluxes from each failed canister to be superimposed.

II.A.2. Computation

An existing code titled Transport-to-Biosphere (TTB) was developed to model nuclide transport in arbitrary-length decay chains from dissolving high-level waste (HLW) glass.[6] It is based on the non-volatile advection dispersion equation for a saturated system comprised of bedrock and parallel planar fractures. The analytical simplifications used by the code require the waste forms and their surrounding buffers to be modeled as spherical equivalents that preserve interfacial surface area. This is necessary for conserving the effect of diffusive mass transport.

The migration of radionuclides through the buffer is determined solely by molecular diffusion. Dispersion (D^L) and diffusion (D^*) processes are assumed to ensure the complete mixing of solutes in the water. Direct infiltration from the buffer surface to the rock matrix is ignored, which causes a steep concentration gradient into the rock beyond the alluvial entrance. This assumption allows for the flux of nuclides at the surface of the buffer to act as the boundary condition for the fracture.

The coefficient of longitudinal dispersion is assumed to be common for all elements, whereas buffer diffusion is modeled as a variable parameter (see section II.C). Bentonite retards the movement of nuclides relative to GW flow according to the following factor:

$$K_{e(k)} = 1 + \rho_b K_{d,b}^{e(k)} (1 - \epsilon_b)/\epsilon_b \quad (1)$$

where ρ_b is the buffer density, ϵ_b is the porosity, and $K_{d,b}^{e(k)}$ is the sorption distribution (or partition) coefficient of the element. K_d is assumed to be a linear isotherm governing the distribution of solid and dissolved phases.

Advection and dispersion are assumed to take place along the axis of the fracture, whereas transverse dispersion is ignored. While in the fracture, nuclides also undergo diffusion into the host rock perpendicular to the axis. The capacity factor for the rock is analogous to the retardation factor of the buffer, and is defined as:

$$\alpha_{e(k)} = \epsilon_p + \rho_p (1 - \epsilon_p) K_{d,p}^{e(k)} \quad (2)$$

where $K_{d,p}^{e(k)}$ is distinct from $K_{d,b}^{e(k)}$ by virtue of having a different geochemistry. Within the rock matrix, transport is strictly diffusive, and the molecular diffusion coefficient couples the analytical model for the fracture to that of the rock matrix. This is defined in terms of the rock porosity, tortuosity τ_p, and diffusion coefficient of the element as measured in free water:

$$D_{e(k),p}^{*} = \epsilon_p \tau_p D_{e(k)} \quad (3)$$

II.A.3. Release Mode

TTB allows the imposition of congruent-release or solubility-limited boundary conditions. Given the low solubility and numerical dominance of uranium atoms in the UO_2 fuel, the release of U will certainly be solubility-limited. That is, a precipitate will form uniformly on the surface of the waste and then dissolve into the EBS when the concentration gradient allows for it. However, given the emphasis on a vitrified waste matrix, the assumptions in TTB effectively separate the mass-release behavior of the waste type and radionuclides contained within. This causes unrealistic uranium isotope proportions in the results when using the solubility-limited boundary condition.

To adapt to this unforeseen limitation of the code, a leach period of 2.5 billion years was set as calculated for

an extremely high solubility and low K_d of uranium. All actinides were then assumed to be congruently released according to the uranium release rate under those conditions.

II.B. Nuclides of interest

The elements of interest in this study are those whose isotopes are fissile or give rise to fissile isotopes through radioactive decay. In general, focus lies on the uranium isotopes U-233 and U-235 and plutonium isotopes Pu-239 and Pu-241.

For ease of calculation, engineering-informed decisions were made to exclude most isotopes in the decay chains with miniscule quantities and half-lives shorter than the expected failure time of 1000 years. The final decay chains chosen for TTB calculation consist of five different actinides, which are grouped by the common nomenclature as follows:

4n: Pu-240 → U-236

4n+1: Cm-245 → Pu-241 → Am-241 → Np-237 → U-233

4n+2: Cm-246 → Pu-242 → U-238 → U-234

4n+3: Am-243 → Pu-239 → U-235

The far-field precipitate will largely consist of uranium isotopes given their preeminence in the UO_2 fuel; therefore, for computational ease, results for uranium will only be included, where U-233 and U-235 govern the total fissile content. Nonetheless, all transuranic (TRU) precursor contributions are factored into the calculation.

II.C. Parameter variation

The variation in transport parameters is shown in TABLE I in terms of lower and upper bounds observed in the literature.[6]–[11]

Variation in the free-water diffusion of the actinides is not considered to be significant and is chosen to be a constant 2.0E-2 m^2/yr. This constant was used to calculate rock matrix diffusion via Eq. (3), whereas effective diffusion in the buffer was chosen to be a sampled quantity. The ranges of K_d values for both the buffer and rock correspond to granitic GW samples tested in both fresh and saline reducing environments with high pH values. The dependence on these geochemical conditions is conservative as they allow uranium species to be mobile, which would enhance the magnitude of the eventual precipitate.

The dependence of porosity on dry density is ignored to decouple the terms in the model. The ranges shown in the table correspond to total void space, both interconnected and closed. The upper range of rock porosity effectively corresponds to a heavily fractured sample.

By Darcy's Law, GW velocities are dependent on the hydraulic gradient in the host rock. Without site-specific information, the bounds included in the table are experimental. Furthermore, unlike K_d, the dependence of solubility on salinity, pH, and other geochemical aspects is decoupled and the ranges included may represent a wide selection of environments.

TABLE I. Ranges of variable parameters

Parameter		Lower Bound	Upper Bound	Unit
GW velocity (v)		0.1	100	m/yr
Rock Porosity (ϵ_p)		0.001	0.5	
Buffer Porosity (ϵ_b)		0.17	0.48	
Fracture Aperture ($2b$)		1.00E-4	1.10E-3	m
Solubility C^*	U	9.6E-8	1.0E-5	mol/m^3
	Np	1.0E-9	1.0E-5	
	Pu	1.0E-11	1.0E-5	
	Am	1.0E-6	1.0E-4	
	Cm	1.0E-6	2.8E-4	
Rock Matrix $K_{d,p}^{e(k)}$	U	1.0E-4	1.0E+2	kg/m^3
	Np	1.0E-3	1.0E+2	
	Pu	2.5E-2	2.5E+1	
	Am	1.0E-2	2.5E+1	
	Cm	1.0E-2	2.5E+1	
Buffer $K_{d,b}^{e(k)}$	U	4.1E-3	1.0E+2	kg/m^3
	Np	6.7E-3	1.0E+2	
	Pu	6.6E-2	5.7E+1	
	Am	2.1E-1	1.0E+1	
	Cm	2.1E-1	1.0E+1	
Effective Buffer $D_{e(k),b}^*$	U	1.6E-4	2.1E-2	m^2/yr
	Np	1.6E-4	2.1E-2	
	Pu	1.6E-4	2.1E-2	
	Am	1.6E-4	7.3E-3	
	Cm	1.6E-4	7.3E-3	

III. METHODOLOGY

III.A. Repository Layout

The characteristics of fuel from the three damaged cores are shown in TABLE II, along with quantities based on averaged fuel characteristics. The average fuel type will be analyzed in this paper to remove considerations of a repository with multiple fuel types.

Canister loadings are based on a maximal subcritical mass, which is 0.303 MT of waste per canister on average. To account for the 257 MT source term, 962 canisters of the averaged fuel would be needed, which can be approximated by a 31 by 31 array. The square format is assumed to neglect specific layout effects as much as possible. In reality, a granitic repository could have multiple tunnels with particular arrays determined by the constraints of the site. Condensing the whole repository into one planar array is a conservative measure to minimize the set of fracture transport distances as much as possible. It is likely that other HLW would be co-disposed in the same repository, however such wastes are not considered to isolate the unique effects from the damaged fuel.

TABLE II: Data for three damaged cores from Fukushima Daiichi and ORIGEN data for 1050-year failure 1point when transport analysis begins.

Data	Core 1	Core 2	Core 3	Total	Avg Core
Maximum waste per canister [MT] (keff=0.98)	0.358	0.282	0.2695	-	0.303
Maximum heavy metal per canister [MT]	0.315	0.248	0.237	-	0.267
Mass of heavy metal in fresh fuel [MT] †	69	94	94	**257**	257
Estimated number of canisters	219	379	396	994	961*
Data at canister failure (50+1000 yr interim cooling)					
Enrichment (U-233+U-235)/U [wt.%]	1.68%	1.88%	1.87%	-	1.82%
Enrichment bound (U precursors added) [wt.%]	2.24%	2.39%	2.46%	-	2.37%
(U-233+U-235+Pu-239+Pu-241)/Heavy Metal [wt.%]	2.07%	2.24%	2.30%	-	2.21%
Uranium content [MT]	66.7	91.1	91.2	249.	83.0
Transuranics content [MT]	0.499	0.617	0.728	1.85	0.615

* total canisters in square array based on average core characteristics for 257 MT source term
† ref [1]

The fuel is assumed to be cooled for an interim period of 50 years prior to emplacement, and all packages are assumed to fail concurrently 1000 years afterwards. The inventories at failure are calculated using the ORIGEN2 point-depletion code as part of the SCALE 6.1 package.[12]

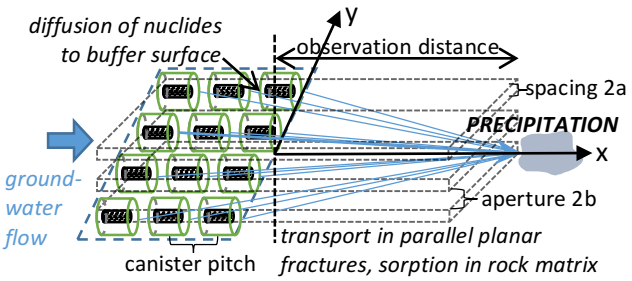

Fig. 1. Schematic of abstract repository intersected by fractures.

Specific parameters relating to the repository are summarized in TABLE III. The buffer thickness and canister diameter are based on the Japanese design for PWR UNF,[13] whereas the one meter height is borrowed from typical dimensions for HLW drums. The canister components are assumed to pose no mass-transfer limitations.

The ten-meter observation distance is chosen to be close to the repository edge (one half-pitch) as a conservative measure. The transport distances from each discrete waste form all lead to this point on the x-axis (see Fig. 1).

III.B. Sampling

III.B.1. Approach

Four different distribution types are considered in the study along with fixed values. The uniform and log-uniform distributions both encompass the lower the upper bounds. The uniform distribution uses evenly-spaced intervals for the probability distribution functions (PDFs) while the log-uniform uses even-spacing on the log base 10 scale (although the distribution itself is based on the natural log with base *e*).

Normal and log-normal distributions were created using the Marsaglia polar method from Box-Muller standard normals. Random numbers were generated using the built-in subroutine in GNU Fortran,[14] where the random seeds were changed automatically with each use. A hundred thousand samples were generated for each distribution.

For the normal distribution, the mean was taken to be the arithmetic average, while the variance was chosen assuming that the upper and lower bounds comprised 95% of all samples, or two standard deviations from the mean. The log-normal distributions used the average of the natural logarithms of the lower and upper bounds as the location parameter. The scaling parameter was iterated manually to provide a 95% confidence interval between the upper and lower bounds.

The PDFs were based on histograms divided into 5000 bins. These were bounded by the minimum (non-negative) and maximum sample values generated for the distribution,

TABLE III. Canister and repository parameters.

Item	Value
Uranium oxide density [kg/m^3]	10,960
Canister height (H_c) [m]	1.000
Canister radius (r_c) [m]	0.419(5)
Buffer thickness (t_b) [m]	0.700
TTB spherical equivalent fuel radius (r_f) [m]	0.546
TTB spherical equivalent buffer radius (r_b) [m]	1.089
Repository array	31 by 31 (961 total)
Array orientation	xy plane
Accumulation direction	x axis
Observation distance from repository edge [m]	10

which removed the need to incorporate infinity into sampling.

A Fortran code was written to generate LHS samples for each of the distributions considered. For variable parameters, 100 divisions of equal probability within the cumulative distribution functions (CDFs) were determined based on the discrete intervals of the PDF. The fineness provided by the 5000 bins proved suitable enough to reduce error with the CDF below 0.1% on average, making this methodology acceptable. For each equal-probability interval, a sample from the distribution was chosen at random using a unique set of random numbers between zero and one.

III.B.2. Parameter Distributions

TABLE IV. Fixed parameters and variable parameters with distributions types for sample variation

Parameter	#1	#2	#3
Leach period (T_L) [yr]	2.509E+9		
Fracture spacing ($2a$) [m]	1 [15]		
Rock density (ρ_p) [kg/m^3]	2600 [16]		
Rock tortuosity factor (τ_p)	0.055 [17]		
Bentonite density (ρ_b^{wet}) [kg/m^3]	2100 [17]		
Fracture material porosity (ϵ_f)	1		
Fracture material density (ρ_f) [kg/m^3]	0		
Waste canister pitch [m]	20		
Longitudinal dispersion (D^L) [m^2/yr]	1		
GW velocity (v) [m/yr]	N		
Rock porosity (ϵ_p)	U		
Buffer porosity (ϵ_b)	U		
Fracture aperture ($2b$) [m]	N [10]		
Rock $K_{d,p}$ [m^3/kg]	LN	N	LU
Buffer $K_{d,b}$ [m^3/kg]			
C^* [mol/m^3]			
Buffer diffusion ($D^*_{e,b}$) [m^2/yr]			

N: normal; U: uniform; LN: log-normal; LU: log-uniform

Log-normal distributions are known to fit experimental data for uranium solubility and its K_d in granite with reasonable accuracy.[8] Nonetheless, three cases are examined in this study that vary based on the manner in which the partition coefficient K_d, solubility C^*, and buffer diffusion $D^*_{e(k),b}$ are sampled. These parameter distributions, along with some constant values, are shown in TABLE IV.

The porosities of the bentonite and rock are sampled uniformly, although the densities are maintained as 2100 and 2600 kg/m^3, respectively. It should be repeated that effective diffusion in the rock matrix is governed by Eq. (3), which depends on two constants and the uniformly-sampled rock porosity, making the parameter itself effectively uniformly-sampled.

Fracture apertures are known to vary similar to a normal or log-normal distribution, although there is no consensus form the literature. Samples are made according to a normal distribution in this study and then halved for evaluation in TTB, as the repeated planar analytical model is with respect to the half-aperture.

The groundwater velocity employed in TTB is an averaged linear velocity. On the microscale, the velocity of water flowing through a pore space varies depending on the flow paths constructed by particles of various sizes. This causes a lack of congruency between the speed of groundwater and a dissolved solute or tracer. The solute is driven by a concentration gradient in conjunction with advective flow, and the groundwater flow path is limited by a pore space that is randomized due to distributions in particle sizes and shapes. Furthermore, the solute may interact with the solid particles chemically and physically and be subject to local changes in groundwater density and viscosity.[18] This dispersion effect of the solute is realized macroscopically through the spreading of the concentration breakthrough curves for the porous medium at a point in space.

Since dispersion is essentially the large-scale indicator of many random variations in the fluid velocity, the velocity is assumed to vary according to a Gaussian distribution as a result of the central limit theorem (see Fig. 2). Although this approach would be sufficient to model dispersion, the coefficient is still maintained as D^L=1 to ensure the Péclet number remains in the advective region.

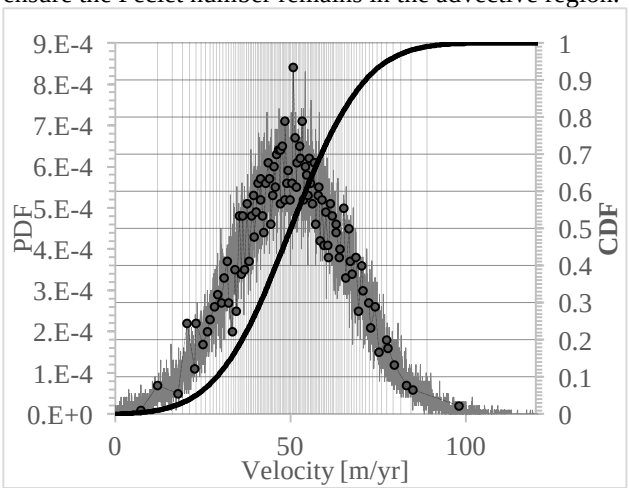

Fig. 2. Distribution of GW velocities shown with 100 equal probability intervals and LHS samples (●).

IV. RESULTS

Data for each time point for each nuclide for each case was taken as the average of all 100 LHS sample and the error was taken to be the standard deviation of those samples. For the total mass and enrichment, these errors were propagated based on the sums and ratios involved. The enrichment is assumed to be the mass ratio of both U-233 and U-235 relative to all uranium isotopes.

IV.A. Total Mass of Far-Field Precipitate

The total superimposed precipitate from all 961 canisters is plotted over time (after canister failure) for the three cases in Fig. 3 along with error bands. Per given point in time, the precipitate in case 3 is larger than that of case 1, and that of case 1 is larger than that of case 2. General behavior for cases 1 and 3 become similar at long times.

Within a hundred million years, 10 MT of uranium cannot be accumulated even within the error margins, although a maximum of 8 MT is within error for case 3. As shown in TABLE V, it takes about 5 million years in case 3 to reach 0.1 MT and 30 million years to reach 1 MT. In case 2, no precipitate indicative of criticality will accumulate until about 70 million years.

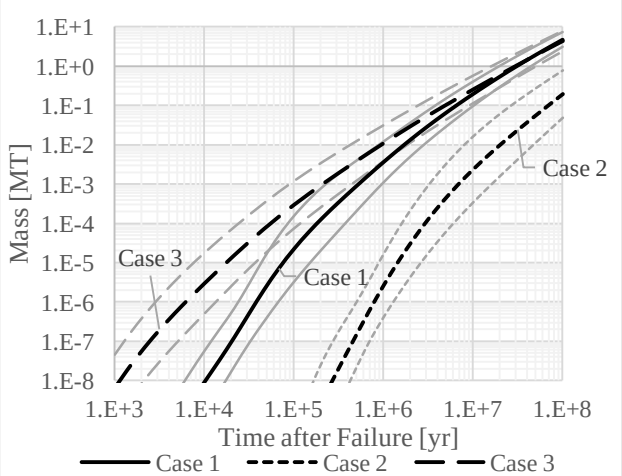

Fig. 3: Total uranium mass in the far-field over time along with error bands for the three cases.

TABLE V. Times of accumulation for certain masses, along with enrichments within the time error.

		Case 1	Case 2	Case 3
0.1 MT	t (10^6 yr)	6.48±2.68	68.6±42.5	4.85±2.43
	En [wt%]	2.24±0.03	2.14±0.19	2.25±0.03
1 MT	t (10^6 yr)	30.7±10.9	-	29.5±13.6
	En [wt%]	2.20±0.03	-	2.21±0.04

IV.B. U-235 Behavior

The isotope U-235 is the most abundant fissile species of interest and accumulates in a different manner for each of the three cases. Fig. 4 shows the CDFs of U-235 accumulation at 6.8 million years normalized to the original 4.53 MT contained in all the canisters at failure. This time point was chosen for being relevant to the masses in TABLE V.

The case 2 CDF is significantly different from the other two and shows that smaller masses are vastly more probable at this point in time and space. Its 99-percentile is roughly an order of magnitude lower than those for the other two cases (see TABLE VI).

The CDF's for case 1 (log-normal) and 3 (log-uniform) are similar, where the median value for #1 is higher but it 95-percentile is marginally lower. A crossover in cumulative probability is observed at 60% for the 0.04% accumulation point. Similar data trends are observed for analogous cases in Fig. 3.9 of Ref [8].

The bulge in the case 3 curve may be an array-based effect whereby Pu-239 has similar mobility to uranium. This allows canisters further away from the precipitate location to contribute more decay-generated U-235 in a lesser amount of time, particularly when compared to case 1.

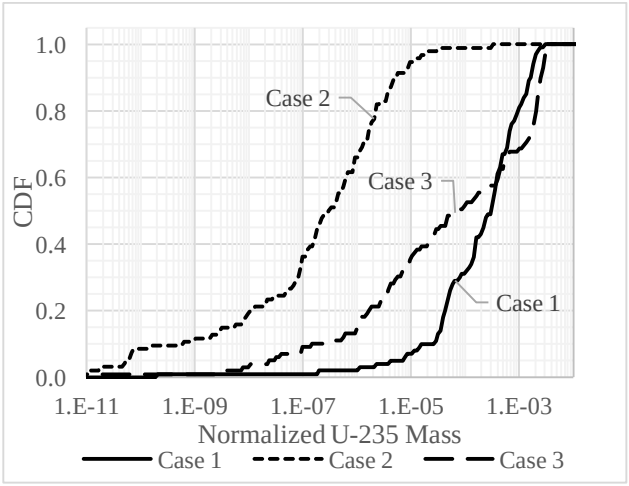

Fig. 4. CDFs of normalized U-235 mass in the far-field for all three cases, as evaluated at 6.8 million years.

TABLE VI. Statistics for normalized mass of U-235 in the far-field.

	Case 1	Case 2	Case 3
5-percentile	6.64E-06	5.07E-11	2.27E-08
Median	2.89E-04	2.87E-07	7.19E-05
95-percentile	1.81E-03	1.03E-05	2.73E-03
99-percentile	2.37E-03	2.84E-04	3.05E-03

IV.C. Enrichment

Fig. 5 shows the evolution of the (U-233+U-235)/U ratio over time and the ranges of uncertainty. At 1000 years, a value of 1.83 wt% is observed for cases 1 and 3, which is near the value observed at canister failure (see TABLE II). The case 3 curve temporarily surpasses #1 in 20,000 years as contributions from transuranics are realized. At 300,000 years, behavior for both becomes identical as the plume of U-238 dominates and begins diluting the enrichment. The peak before dilution is 2.27 wt%, where a maximal 2.32 wt% is within error (although corresponding to fractions of a kilogram of uranium). As shown in TABLE V, the representative masses correspond to enrichments after the peak values.

At early times, case 2 begins with very high enrichments due to fissile precursors that are much more mobile than uranium. For these high enrichments, the correspondingly miniscule total masses from Fig. 3 imply that these accumulations are not indicative of criticality.

Only until 300,000 years after failure does the arriving plume of U-238 cause the general behavior fall in line with the other cases, albeit with the greatest breadth of uncertainty. At very long times, enrichment for case 2 is prone to be the largest given the high TRU mobility.

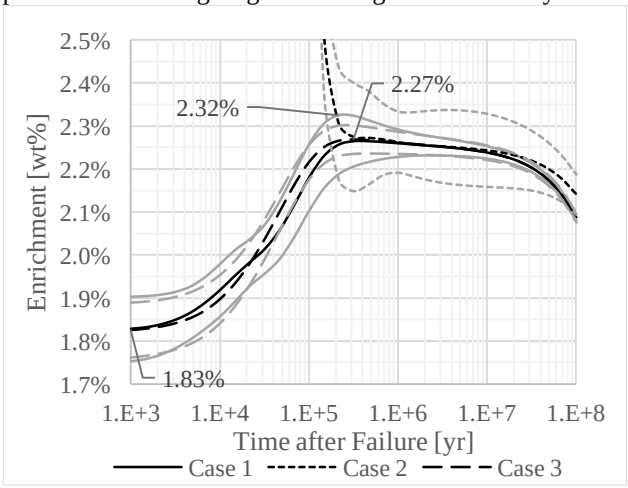

Fig. 5. (U-233+U-235)/U ratio behavior over time for all three cases along with uncertainty bands.

V. DISCUSSION

The parameters for case 3, in which a log-normal distribution is employed for key transport quantities, appears most prone to larger accumulations of uranium in the far-field per given point in time. Within the band of uncertainty, 0.1 MT can precipitate as soon as 2.5 million years and 1 MT in 16 million years.

The case 1 parameters employing log-uniform distributions result in heavier retardation of TRU precursors compared to case 3, leading to lower precipitate masses. This is caused by larger K_d values having equal probabilities of being sampled compared to smaller log-scale values. Smaller U-235 masses have greater probability of being observed in case 3 through the decay of mobile Pu-239. Larger U-235 masses are most probable in case 1 as indicated by the higher median value, which mainly corresponds to the original plume of uranium released from the buffer into the fracture. Nonetheless, in the wider perspective, enrichment behavior over time is more-or-less identical for these two cases even within the bands of uncertainty.

The case 2 parameters resulted in the most significant retardation of uranium isotopes relative to its precursors. By the methodology employed for the normal distribution, this may have been caused by a bias towards the upper bounds of K_d for uranium since smaller values on the log scale were not as probable. As a consequence, the long-term enrichment behavior is more paramount in this case as more Np-237 and Pu-239 decay contributions are realized. On the same time scale required for the case 2 parameters to precipitate 0.1 MT, the other two cases can accumulate more than 1 MT with enrichments above 2 wt%.

The 2.21±0.04 wt% enrichment figure for the 1 MT precipitate of case 3 is within error of the 2.25 wt% modeled in the neutronics simulations of Ref [3]. It can be assumed that the trends for critical masses do not change drastically for a 0.04 wt% difference in enrichment, and that the precipitate location is in fracture sandstone. Using the results of these simulations, the precipitate would need to accumulate in a configuration with an averaged fracture volume of at least 26%, where around 8% of the fracture is occupied by uranium metal, in order for the deposition to be critical. According to this transport analysis, such a deposition can occur between 16 and 43 million years. The 0.1 mass can be achieved within ten million years, but the exact configuration needed for such a small mass to be critical is unknown.

VI. CONCLUSIONS

If the safety assessment of a repository for FD damaged fuel is extended to the tens of millions of years, a critical mass in the far-field resulting from extensive waste package failure cannot be excluded from consideration. An analysis is recommended for the thermo-hydro-mechanical and chemical consequences of critical accumulation. If such an analysis were to show that the role of the bedrock as a barrier is not impacted by criticality, then the assessment could move on to other scenarios for safety evaluation.

It should be noted that the magnitudes of precipitates observed in the results are less liable to occur if the range of solubilities is strictly limited to a reducing granitic environment. With such restrictions in place, the upper bounds in TABLE I would be heavily reduced and severely impact the ability for uranium to reach the precipitation location per given point in time.

Cases in future calculations can vary the distributions of the four main transport parameters as opposed to keeping them uniform, e.g. a case with a distribution promoting the lower range of solubilities and one favoring higher K_d. The dispersion coefficient can also be set to zero in favor of modeling this effect via sampling the GW velocity from a normal distribution. Furthermore, for comparison, a case can be made where this velocity is fixed, allowing the concentration plume to be more representative of a fixed (as opposed to diffused) front.

Given the range of rock matrix porosities, from values indicative of fine micropores to those indicative of fissured samples, the uniform approach used in this study may have favored higher values. This would effectively bias the capacity factors and diffusion coefficients towards higher values, and it is not certain whether the combined effect adheres to the conservative framework. A future study should test log-uniform sampling of these porosities to probe the effect of low porosity, impervious rock.

In terms of the effects of using an array of discrete waste forms as opposed to a point source or continuous planar source, data is affected primarily by the resulting collection of transport distances. When analyzing decay chains of nuclides with different degrees of mobility, these distances introduce lags in the superposed mass data that wouldn't be seen in other studies. Series of LHS analyses can be based on adjusting both the pitch distance (and even the observation distance beyond the repository edge) to further evaluate this effect.

Finally, given the limitations of the TTB code in evaluating the solubility-limited release for UO_2 fuel, a similar model should be developed that better characterizes the boundary conditions at the fracture entrance. If uranium release remains solubility-limited, then the precipitation figures are sure to be impacted significantly.

ACKNOWLEDGMENTS

This paper includes a part of the result obtained in the work for "study for criticality safety after disposal" based on the budget of countermeasures for decommissioning and contaminated water treatment in 2014JFY. Those were entrusted to International Research Institute for Nuclear Decommissioning (IRID) from Minister of Economy, Trade and Industry (METI) and conducted by Japan Atomic Energy Agency as a member of IRID.

REFERENCES

[1] K. Nishihara, H. Iwamoto, and K. Suyama, "Estimation of Fuel Compositions in Fukushima-Daiichi Nuclear Power Plant," JAEA-Data/Code 2012-018, 2012.

[2] J.-H. Ahn, "Criticality Safety of Geologic Disposal for High-Level Radioactive Wastes," *Nucl. Eng. Technol.*, vol. 38, no. 6, pp. 489–504, 2006.

[3] X. Liu, J. Ahn, and F. Hirano, "Conditions for criticality by uranium deposition in water-saturated geological formations," *J. Nucl. Sci. Technol.*, no. ahead-of-print, pp. 1–10, 2014.

[4] J. Ahn, S. Armel, J. Burch, P. L. Chambré, E. Greenspan, and D. A. Roberts, "Underground Autocatalytic Criticality from Fissile Materials Solidified in Borosilicate Glass," *PNC ZA*, vol. 995, pp. 96–1, 1997.

[5] "H12: Project to Establish the Scientific and Technical Basis for HLW Disposal in Japan, Project Overview Report," Japan Nuclear Cycle Development Institute, Japan, JNC TN1410 2000-001, Apr. 2000.

[6] J. Ahn, "Integrated radionuclide transport model for a high-level waste repository in water-saturated geologic formations," *Nucl. Technol.*, vol. 121, no. 1, pp. 24–39, 1998.

[7] F. Surma and Y. Geraud, "Porosity and Thermal Conductivity of the Soultz-sous-Forêts Granite," in *Thermo-Hydro-Mechanical Coupling in Fractured Rock*, H.-J. Kümpel, Ed. Birkhäuser Basel, 2003, pp. 1125–1136.

[8] J. Ahn, S. Kuo, D. A. Roberts, and P. L. Chambré, "Release of radionuclides from multiple canisters in a high level waste repository," UCB-NE-4221, 1998.

[9] S. Kaufhold, M. Plötze, M. Klinkenberg, and R. Dohrmann, "Density and porosity of bentonites," *J. Porous Mater.*, vol. 20, no. 1, pp. 191–208, Feb. 2013.

[10] E. Hakami and E. Larsson, "Aperture measurements and flow experiments on a single natural fracture," *Int. J. Rock Mech. Min. Sci. Geomech. Abstr.*, vol. 33, no. 4, pp. 395–404, Jun. 1996.

[11] Joonhong Ahn, Ehud Greenspan, and Paul L Chambre, "Mechanisms and Possibility of Autocatalytic Criticality by High-Level Wastes Buried in Water-Saturated Geologic Formation," *Nucl. Back-End Res.*, vol. 4, no. 2, pp. 3–20, 1997.

[12] B.T. Rearden and M.A. Jessee, *SCALE Code System*. Oak Ridge, TN: Oak Ridge National Laboratory, 2016.

[13] Japan Atomic Energy Agency, "The specifications of engineering barrier system for direct disposal of spent fuels and burnup calculation condition," JAEA-Research 2015-2016.

[14] *GFortran, GNU Compiler Collection (GCC)*. GNU.

[15] "Technical Report on Research and Development for Geological Disposal of High-Level Radioactive Wastes," Power Reactor and Nuclear Fuel Development Corporation, PNC TN 1410 92-08, 1992.

[16] D. W. Waples and J. S. Waples, "A Review and Evaluation of Specific Heat Capacities of Rocks, Minerals, and Subsurface Fluids. Part 1: Minerals and Nonporous Rocks," *Nat. Resour. Res.*, vol. 13, no. 2, pp. 97–122, Jun. 2004.

[17] J.-H. Ahn, T. Ikeda, and T. Ohe, "Quantitative performance allocation of multi-barrier system for high-level radioactive waste disposal," 1995.

[18] J. Bear, *Dynamics of fluids in porous media*. Courier Corporation, 2013.